

## Paper IV



## **Antiviral Effects of Artesunate on JC Polyomavirus Replication in COS-7 cells**

Biswa Nath Sharma<sup>1,2</sup>, Manfred Marschall<sup>3</sup>, and Christine Hanssen Rinaldo<sup>1,4,#</sup>

<sup>1</sup>Department of Microbiology and Infection Control, University Hospital of North Norway, Tromsø, Norway,

<sup>2</sup>Department of Medical Biology, UiT The Arctic University of Norway, Tromsø, Norway

<sup>3</sup>Institute for Clinical and Molecular Virology, University of Erlangen-Nuremberg, Germany

<sup>4</sup> Metabolic and Renal Research Group, UiT The Arctic University of Norway, Tromsø, Norway

Corresponding author:

Christine Hanssen Rinaldo

Department of Microbiology and Infection Control

University Hospital of North Norway, P.O. Box 56, N-9038 Tromsø

Phone: +47 77 75 58 64

Fax: +47 77 62 70 15

e-mail: [christine.rinaldo@unn.no](mailto:christine.rinaldo@unn.no)

Running title: Artesunate Inhibits JC Polyomavirus Replication

## ABSTRACT

The human JC polyomavirus (JCPyV) causes the fatal demyelinating disease progressive multifocal leukoencephalopathy mainly affecting immunosuppressed individuals. Unfortunately, no effective antiviral therapy is presently available for the treatment of JCPyV infections. The aim of this study was to investigate the anti-JCPyV effect of the antimalarial drug artesunate. The permissivity for JCPyV MAD-4 was first compared in four cell lines, and the monkey kidney cell line COS-7 was selected. Artesunate caused a concentration-dependent decrease in extracellular JCPyV DNA load with an  $EC_{50}$  of 3.0  $\mu$ M at 96 hours postinfection. This effect correlated with inhibition of the expression of the major capsid protein VP1, and the production and release of infectious viral progeny. For concentrations below 20  $\mu$ M, a transient reduction in DNA replication and cell proliferation was seen, while for higher concentrations some cytotoxicity was detected. Interestingly, the JCPyV-infected cells were more sensitive to the cytostatic effect of the drug than the mock-infected cells. A selective index of 15 was found when cytotoxicity was calculated based on cellular DNA replication. In conclusion, artesunate is efficacious in inhibiting JCPyV replication at micromolar concentrations and the inhibition probably reflects an effect on cellular proteins and involves transient cytostatic effects.

## INTRODUCTION

Progressive multifocal leucoencephalopathy (PML) is a rare and usually fatal demyelinating disease caused by the lytic replication of JC polyomavirus (JCPyV) in oligodendrocytes (1). The disease mainly affects individuals afflicted with HIV-AIDS or patients undergoing treatment with certain immunomodulatory monoclonal antibodies but can also affect transplant patients, patients with hematological diseases or idiopathic CD4 T-cell lymphocytopenia (2, 3). A few cases of PML in immunocompetent persons have also been described (4, 5). Infrequently JCPyV causes other diseases affecting the central nervous system (CNS) or kidneys (reviewed in (2)). Infection with JCPyV is very common and by adulthood about 70% of all individuals are infected (6-8). After subclinical primary infection, JCPyV remains latent in the renourinary tract and possibly in the brain and lymphoid organs (9-12). Lifelong latency is interspersed by occasional asymptomatic reactivation with shedding in urine (6, 7).

JCPyV belongs to the family *Polyomaviridae*, genus *Orthopolyomavirus* (13). JCPyV is a non-enveloped virus with a 5 Kb circular double stranded DNA genome that can be divided into 3 major regions: the non-coding control region (NCCR), the early region encoding the regulatory proteins small T-antigen (sTag), large T-antigen (LTag) and the derivatives T'135, T'136 and T'165; and the late region encoding the viral capsid proteins VP1, VP2 and VP3 and the agnoprotein, whose function remains elusive (14). The NCCR of JCPyV found in the cerebrospinal fluid (CSF) or the brain of PML patients is typically rearranged with deletions and insertions compared to the archetype virus shed in urine by healthy individuals. Interestingly, in cell culture the rearranged viruses usually express higher levels of early gene products and have a higher replication potential than archetype virus (15).

Although human primary oligodendrocytes would be the most pathophysiologically relevant *in vitro* model for PML, these cells are difficult to propagate. Besides primary human fetal glial (PHFG) (1, 16) and human brain progenitor-derived astrocytes (PDA cells) (17), few human primary cell types have been permissive for JCPyV (reviewed in (2)). Most JCPyV studies have therefore been performed in simian virus 40 (SV40) immortalized cell lines expressing SV40 LTag like the African monkey kidney cell line COS-7 (18, 19), the human embryonic kidney cell line HEK 293TT (20, 21), which probably is of neuronal lineage (22), and the human fetal glial cell line SVG (23). Of note, the SVG p12 cell line from ATCC was recently found to be contaminated with the closely related BK polyomavirus (BKPyV), but the frequently used subclone SVG-A may serve as a BKPyV-negative alternative (24).

Though a number of drugs have been explored *in vitro* and in a limited number of patients, no anti-JCPyV drug with proven efficacy is yet available (reviewed in (2)). Artesunate, the preferred drug for treatment of severe malaria (25), has shown broad antiviral activity *in vitro* (26-31). Apparently it was successfully used for treatment of four transplant patients with recurrent multiresistant cytomegalovirus (CMV) infection (32, 33) and one child with a human herpesvirus 6 infection (34) but did not give satisfactory results in other patients (33, 35, 36). Recently, we reported that artesunate has antiviral activity against BKPyV in human primary renal proximal tubular epithelial cells (RPTECs). The antiviral effect is connected to transient cytostatic effects without cytotoxicity (37). Encouraged by the good safety profile and low incidence of side effects found in numerous studies with artesunate, we decided to investigate its effects on JCPyV replication. We started by comparing the permissivity for JCPyV MAD-4 in COS-7, HEK 293TT, SVG-A, and M03.13 cells, the latter an immortalized human-human hybrid cell line with phenotypic characteristics

of primary oligodendrocytes (38). Here we show that COS-7 is the best suited cell line for JCPyV MAD-4 replication studies and that artesunate inhibits the replication of JCPyV MAD-4 in COS-7 cells by a mechanism closely connected to its transient cytostatic effect.

## **MATERIALS AND METHODS**

### **JCPyV MAD-4 propagation**

The experiments were performed with JCPyV MAD-4 (ATCC VR-1583), a viral strain with a rearranged NCCR originally isolated from the brain of a PML patient (39) and previously used for antiviral studies (17).

The plasmid pGEMMAD-4, containing the complete JCPyV MAD-4 genome in a pGEM3Zf(+) vector (15) was kindly provided by Dr. Hans H. Hirsch, University of Basel, Switzerland. To generate infectious JCPyV MAD-4, the plasmid pGEMMAD-4 was cleaved by EcoRI and the complete JCPyV genome was religated and transfected into COS-7 cells using lipofectamine 2000 (Life Technologies) as previously described (15). The supernatant was replaced by fresh medium at 7 days posttransfection and at 14 days posttransfection infectious virus was harvested by 6 cycles of freezing and thawing, followed by centrifugation at 900 rpm for 5 minutes to clarify the supernatants. To produce more virus, the first passage of JCPyV MAD-4 was used to infect new COS-7 cells. The medium was changed 7 days postinfection (dpi) and at 14 dpi, the supernatant containing JCPyV MAD-4 at a viral load of  $2.14 \times 10^{10}$  genomic equivalents (GEq)/ml was harvested. The supernatant was diluted in 1:3 in the medium and was used to infect cells in all experiments shown.

### **Cell propagation**

The human embryonic kidney cell line HEK 293TT (20) was propagated in Dulbecco's modified Eagle's medium (DMEM) (D5796, Sigma) with sodium pyruvate (100mM) and 10% fetal bovine serum (FBS). The human fetal glial cell line SVG-A



(23, 40) that was kindly provided by Dr. Walter Atwood, Brown University USA, was propagated in MEM (M4655, Sigma) with 10% FBS. The human-human hybrid cell line M03.13 (CELLutions Biosystems Inc) (38), was propagated in DMEM (D5796, Sigma) with 10% FBS as instructed by the supplier. The African green monkey kidney cell line COS-7 (ATCC RL1651) was propagated in DMEM (DMEM-H) (D5671, Sigma) containing 1% Glutamax (equivalent to 2mM L-glutamine) (Life Technologies) and either 10 or 3 % FBS.

### **JCPyV MAD-4 permissivity study**

HEK 293TT, SVG-A, COS-7 and M03.13 cells were propagated in their respective media supplemented with 10% FBS. About 15000 cells per 0.95 cm<sup>2</sup> well were seeded and the next day the approximately 60% confluent cells were infected with 100 µl JCPyV MAD-4 supernatant for 2 h before surplus infectious units were removed; cells were washed once with phosphate buffered saline (PBS) and complete medium was added.

### **Infection and drug treatment**

Artesunate (Saokim, Hanoi, Vietnam) was dissolved in dimethyl sulfoxide (DMSO) to a concentration of 65 mM, and immediately stored in aliquots at -70°C. Prior to use, the stock was diluted in DMEM with 3% FBS to working concentrations. One day before infection 15000 COS-7 cells per 0.95 cm<sup>2</sup> well were seeded in DMEM growth medium containing 3% FBS. The cells were infected with 100 µl JCPyV MAD-4 for 2 h before surplus infectious units were removed, the cells were washed once with

PBS and medium containing 3% FBS with or without increasing concentrations of artesunate was added unless otherwise indicated. A DMSO control matching the DMSO concentration in artesunate 20  $\mu$ M was included in all experiments.

### **Quantitation of extracellular and intracellular JCPyV DNA loads**

To quantitate extracellular JCPyV DNA loads, supernatants were harvested from the artesunate treated JCPyV-infected cells at 24 and 96 hours postinfection (hpi) and stored at -70°C until quantitation by quantitative PCR (qPCR) using primers and probe targeting the JCPyV LTag gene as described elsewhere (17, 41). Shortly before qPCR, supernatants were diluted in distilled H<sub>2</sub>O (1:100) and boiled for 5 minutes. To quantitate intracellular JCPyV DNA load, the DNA was extracted from the cells using the MagAttract DNA mini-M48 kit (Qiagen). In brief, cells were washed once with PBS, lysed by adding G2 buffer and immediately stored at -70 °C until robotic extraction (GenoM-48, Qiagen). The intracellular JCPyV DNA loads were quantitated by qPCR as described for extracellular JCPyV loads but without dilution and boiling. Each experiment had two individual samples and each sample was measured in triplicate.

### **Immunofluorescence staining, microscopy and digital image processing**

The JCPyV MAD-4 infected cells with or without artesunate treatment were fixed at 96 hpi in 4% paraformaldehyde (PFA) for 5 minutes and permeabilized by methanol for 10 minutes before immunofluorescence staining was performed using primary antibodies, a polyclonal rabbit antiserum directed against the C-terminal part of BKPyV LTag (1:1000) (42) and a monoclonal mouse antiserum directed against JCPyV VP1 (1:400) (ab34756, abcam). The BKPyV LTag antiserum cross-reacts with

SV40 LTag and JCPyV LTag. Nuclei were labeled with Draq5 dye (1:1000) (Biostatus). Images were collected using a Nikon TE2000 microscope (10X objective) and processed with NIS-Elements BR 3.2 (Nikon Corporation).

### **Infectious progeny virus release**

The supernatants harvested from untreated and artesunate treated JCPyV MAD-4 infected COS-7 cells at 96 hpi for determination of extracellular JCPyV DNA loads, were diluted 1:2 and were used to infect COS-7 cells. The infection was performed as described above, but this time only growth medium without artesunate was added. At 96 hpi, the cells were fixed and immunofluorescence staining performed as described above.

### **Cell proliferation and cell viability assays**

The proliferation of mock- and JCPyV-infected COS-7 cells with or without artesunate treatment was monitored in real time by the xCELLigence system using a RTCA DP instrument as previously described (43). This system measures the electrical impedance, which is influenced by adhesion, number and size of the cells and expresses this as an arbitrary unit (cell index) that reflects cell proliferation and viability. One day before infection, 6000 cells per 0.2 cm<sup>2</sup> well were seeded in a volume of 200 µl. In order to avoid disturbances of the cell index, supernatants were never completely removed from the wells. In short, 120 µl of supernatant was removed from each well and 80 µl of the JCPyV infectious supernatant (undiluted) was added for 2 h before the infectious surplus was successively removed by a

dilution method of 3 cycles. In each cycle, 150  $\mu$ l of the supernatant was removed and replaced by 150  $\mu$ l of fresh medium. At the end, 100  $\mu$ l of the medium was left in all wells. Thereafter, 100  $\mu$ l of medium with artesunate in double concentration or without artesunate was added. The mock-infected cells were treated the same way. The cell index was measured every 15 min for the first 6 h after seeding and thereafter every 30 min. In addition, cell viability of artesunate treated COS-7 cells was measured by three different endpoint assays as described below. In short, 6000 cells per 0.32 cm<sup>2</sup> well were seeded and the next day the cells were either mock-infected or JCPyV-infected. The cells were infected by incubation with 80  $\mu$ l of the JCPyV infectious supernatant for 2 h. Then, the surplus infectious JCPyV was removed and the cells were treated with increasing concentrations of artesunate. Cellular DNA replication was quantified by a colorimetric measurement of 20 h bromodeoxyuridine (BrdU) incorporation into DNA using the Cell Proliferation ELISA, BrdU assay (Roche). Total cellular metabolic activity was monitored by the colorimetric measurement of 3 h reduction of resazurin dye by mitochondrial, microsomal and cytosolic enzymes using the TOX-8 Assay (Sigma) both according to manufacturer's instructions as earlier described (37, 44). The measurements were performed at 24, 48, 72 and 96 hours posttreatment (hpt) of mock-infected cells and at 96 hpt of JCPyV-infected cells. As an alternative measure of the total cellular metabolic activity, adenosine triphosphate (ATP) content of both mock- and JCPyV-infected cells was measured at 96 hpt by CellTiter-Glo Luminescent Cell Viability Assay (Promega) according to manufacturer's instruction. In short, 100  $\mu$ l of the CellTiter-Glo reagent was added to each well containing 100  $\mu$ l supernatant and the plate was mixed for 2 minutes on a shaker to induce cell lysis. The plate was then

incubated for 10 minutes at room temperature to stabilize the luminescent signal and luminescence was measured using a Tecan Infinite F200PRO reader (TECAN).

The potential cytotoxic effects of artesunate on mock-infected or JCPyV-infected COS-7 cells were measured by the CellTox Green Cytotoxicity Assay (Promega) at 24, 48, 72 and 96 hpt as described by the manufacturer. The assay measures the changes in the membrane integrity of the cell by using a green cyanine dye that is excluded from viable cells and preferentially stains the DNA from dead cells. When the dye binds DNA released from cells, its fluorescence properties are substantially enhanced. According to the manufacturer, signals are stable for at least 3 days and that the same wells can be measured several times. Cell seeding, JCPyV infection and artesunate treatment were carried out as earlier described but this time the green dye was included in the artesunate dilutions in a 1:1000 dilution. The fluorescence activity of the dye was measured at 24, 48, 72 and 96 hpt at an excitation/emission of 485/ 520 nm with 5 flashes using a Tecan Infinite F200PRO reader (TECAN).

### **Selectivity index of artesunate**

As described previously (37) the XLfit program (Fit Model: Dose response one site 210) was used to determine the effective concentration of artesunate giving a 50% inhibition of extracellular JCPyV DNA load ( $EC_{50}$ ) and the 50% cell cytotoxicity ( $CC_{50}$ ) was monitored as inhibition of cellular DNA replication in mock-infected COS-7 cells at 96 hpt. The selectivity index ( $SI_{50}$ ) was calculated by dividing  $CC_{50}$  by  $EC_{50}$ .

## RESULTS

### The replication of JCPyV MAD-4 in different cell lines

In order to find the most permissive cell line for our JCPyV antiviral study, the replication of JCPyV MAD-4 was investigated in COS-7, HEK 293TT, SVG-A and M03.13 cells by comparing the replication of JCPyV DNA, the expression of VP1 protein and the release of JCPyV progeny. Briefly, all cell types were seeded at the same cell density and infected with JCPyV MAD-4 produced in COS-7 cells. At 1, 4 and 7 dpi supernatants and cell lysates were separately collected for determination of extracellular and intracellular JCPyV DNA by qPCR and cells were fixed for immunofluorescence staining. Comparing the extracellular JCPyV DNA load at 7 dpi to that of 1 dpi, the latter representing input JCPyV DNA, a total increase of 0.9, 1.1, and 0.3 log JCPyV DNA was found in supernatants from COS-7, HEK 293TT, and SVG-A, respectively (**Fig.1A**). At the same time, the intracellular JCPyV DNA load increased by 1.5, 1.6 and 0.3 log, respectively (**Fig.1A**). Of note, for both COS-7 and HEK 293TT cells, an increase in intracellular JCPyV DNA load was observed already at 4 dpi. However, for M03.13 cells, there was no increase but rather a decrease in intracellular and extracellular JCPyV DNA at 4 and 7 dpi. Next, immunofluorescence staining was performed using primary antibodies directed against JCPyV VP1 and BKPyV LTag, the latter known to cross-react with SV40 LTag and JCPyV LTag. At 4 dpi, VP1 expressing cells were found in wells of COS-7, HEK 293TT, and SVG-A cells but not in M03.13 cells (**Fig.1B**, red). The highest number of VP1 expressing cells was found in wells with COS-7 cells. As expected, COS-7, HEK 293TT and SVG-A cells all expressed SV40 LTag (**Fig.1B**, green) while no SV40 or JCPyV LTag expression was found in M03.13 cells.

In the experiments described above, the infectious JCPyV was obtained from the monkey cell line COS-7. To investigate if the cellular origin of the virus played a role, the whole experiment was repeated with JCPyV MAD-4 generated in human SVG-A cells. The results showed the same trend as experiments with virus from COS-7 cells (data not shown). Taken together, we concluded that COS-7 and HEK 293TT cells are the most permissive of the tested cells for JCPyV MAD-4 infection and that M03.13 cells apparently are non-permissive for at least this strain of JCPyV. Since we and others have experienced that HEK 293TT cells easily detach and therefore are not very suited for microscopic analysis or studies going over several days (45), we decided to use COS-7 cells for the investigation of artesunate on JCPyV replication. We also decided to use the JCPyV MAD-4 supernatant generated in COS-7 cells (hereafter denoted JCPyV) for all further experiments.

### **Artesunate inhibits JCPyV replication in COS-7**

The one step replication cycle of JCPyV in COS-7 cells grown in medium containing 2% FBS is known to be 4 days (19). Similar to this, a one log increase in extracellular JCPyV DNA load was found at 4 dpi when COS-7 cells were cultured in medium containing 3% FBS (data not shown) but not when 10% FBS was used (**Fig.1A**). We therefore decided to use 3% FBS concentration for all experiments. In order to investigate the antiviral effect of artesunate on JCPyV replication in COS-7 cells, the cells were infected with JCPyV for 2 h and treated with artesunate in concentrations from 0.625 to 80  $\mu$ M until the supernatants were collected for JCPyV qPCR and the cells were fixed for immunofluorescence staining at 96 hpi. To measure the input JCPyV DNA load, supernatants from some untreated wells were harvested already at

24 hpi. The qPCR of the supernatants from the untreated wells showed a 0.9 log increase in extracellular JCPyV DNA at 96 hpi (**Fig.2A**). Addition of artesunate reduced the extracellular JCPyV DNA load in a concentration-dependent manner (**Fig.2A**). While artesunate at 2.5, 10 and 20  $\mu\text{M}$  reduced the JCPyV load by approximately 0.3 log (48%), 0.6 log (75%) and 0.8 log (84%), respectively, higher artesunate concentrations reduced JCPyV almost to the level of input virus. Of note, the DMSO control showed no inhibition of the JCPyV load.

Next, we investigated the effect of artesunate on JCPyV VP1 expression by immunofluorescence staining using the mouse monoclonal JCPyV VP1 antibody. Compared to untreated cells, a concentration-dependent reduction of VP1 expressing cells was detected (**Fig.2B**, red). Of note, microscopy also revealed a slight reduction in cell numbers when 20  $\mu\text{M}$  artesunate was used and a dramatic reduction when 40 and 80  $\mu\text{M}$  artesunate were used (**Fig.2B**, blue).

To investigate whether the inhibitory effect of artesunate on extracellular JCPyV load corresponded to a decline in released infectious JCPyV, the supernatants harvested at 96 hpi were also used to infect new COS-7 cells. After 2 hours of infection the inoculum was replaced with fresh medium without artesunate and the cells were left until 96 hpi when immunofluorescence staining for VP1 was performed. The number of VP1 expressing cells was found to be inversely proportional to the artesunate concentration originally used (**Fig.2C**, red). The results thereby confirmed that artesunate reduced the JCPyV progeny release in a concentration-dependent manner.

We conclude that artesunate inhibits JCPyV replication in COS-7 cells in concentration-dependent manner.



## **Artesunate inhibits cell proliferation of mock-infected and JCPyV-infected COS-7 cells**

Having observed a decreased cell number when artesunate concentrations from 20  $\mu\text{M}$  were used, we wished to investigate the influence of artesunate on cell viability in detail. To analyze the influence of artesunate on both mock-infected and JCPyV-infected COS-7 cells in real-time, the xCelligence system was used. As previously described, this system provides quantitative information about the biological status of the cells, including cell adhesion, numbers, and size. We first compared the status of mock-infected and JCPyV-infected COS-7 cells. The cells were inoculated with conditioned media or JCPyV for 2 h before this was replaced with fresh medium. The cell index was normalized immediately after JCPyV addition. For both mock-infected and JCPyV-infected cells, the cell index was found to gradually increase at least up to 96 hpi suggesting an increase in cell number, size of the cells, attachment or a combination of this (**Fig.3A**). Of note, the cell index was slightly higher in JCPyV-infected than in mock-infected cells and this difference increased over time. Next, the effect of artesunate was investigated on mock-infected and JCPyV-infected cells. As before, the cells were incubated with conditioned medium or JCPyV for 2 h but this was replaced by fresh medium with artesunate to achieve final concentrations from 1.25 to 40  $\mu\text{M}$ . The cell index was normalized immediately after the addition of artesunate but this time the cell index of untreated cells was set as baseline 0. A concentration-dependent decrease in the cell index of artesunate treated cells started from about 7 hpt (**Fig.3B and C**). For mock-infected cells treated with artesunate concentrations below 20  $\mu\text{M}$ , the inhibition was completely reversed about 36-60 h after treatment start where the time to release correlated inversely with the artesunate concentration (**Fig.3B**). Interestingly after reversal of inhibition, cells

treated with artesunate 10  $\mu$ M showed an increased cell index compared to untreated cells. For cells treated with artesunate 20 and 40  $\mu$ M, no reversal of inhibition was seen up to 96 h of treatment (**Fig.3B**) but for 20  $\mu$ M the inhibition was reversed from 125 hpt (data not shown). The results from JCPyV-infected cells were similar (**Fig.3C**). To summarize our results from the XCelligence system, artesunate has a rapid and strong anti-proliferative effect on both mock-infected and JCPyV-infected COS-7 cells but the effect is transient for concentrations less than 20  $\mu$ M.

We next examined the effects of artesunate at concentrations ranging from 0.625 to 80  $\mu$ M on cellular DNA replication and total metabolic activity in mock-infected cells by the use of colorimetric endpoint BrdU- and Resazurin assay in multiplex at 24, 48, 72 and 96 hpt. At 24 hpt, the cellular DNA replication was reduced in a concentration-dependent manner (**Fig.4A**). The largest reductions were found for artesunate 40 and 80  $\mu$ M reducing DNA replication by 16 and 23%, respectively. For these two concentrations, a further reduction, to more than 40 and 70%, respectively, was observed at later time points. In contrast to this, for artesunate concentrations less than 40  $\mu$ M, the strongest inhibition of DNA replication was observed at 24 hpt. The inhibition gradually decreased at 48 and 72 hpt and was completely diminished at 96 hpt. In fact, at 96 hpt, the DNA replication was higher in the artesunate treated wells than in untreated wells. At 24 hpt, the metabolic activity was also reduced in a concentration-dependent manner (**Fig.4B**). The largest reductions were found for artesunate 40 and 80  $\mu$ M, reducing the metabolic activity by 37 and 58%, respectively. For these two concentrations, a further decrease was observed at 48 hpt, leading to a total reduction of about 75 and 90%, respectively. However, no further reduction was seen over the next two days. In contrast to this, the inhibition of

metabolic activity caused by artesunate concentrations less than 40  $\mu\text{M}$ , was not significantly changed over the next three days.

To investigate if the cellular DNA replication and metabolic activity of JCPyV-infected cells were similarly affected, BrdU and resazurin assay were also performed in infected cells at 96 hpt (98hpi) and the results were normalized to untreated mock-infected cells. A concentration-dependent reduction of the DNA replication was found (**Fig.4C**) and at all concentrations above 5  $\mu\text{M}$ , the DNA replication was significantly more affected than in mock-infected cells (**Fig.4A**). The metabolic activity which was slightly higher in JCPyV-infected than in mock-infected cells, was reduced in a concentration-dependent manner (**Fig.4D**) similar to mock-infected cells (**Fig.4B**).

In order to verify the metabolic activity results, the luminescent assay CellTiter-Glo was used to measure the ATP content of mock-infected and JCPyV-infected cells at 96 hpt (98 hpi). The total metabolic activity was found to decrease with increasing artesunate concentrations and the results were therefore similar to results obtained by the resazurin assay (**Fig.4E**). However, with this highly sensitive assay the viable of cells in JCPyV-infected wells was found to be less than in mock-infected wells. The difference was most pronounced in untreated cells, suggesting that this was due to lytic JCPyV replication.

As previously described (37), intracellular LDH can be used as a marker for the number of cells present. When the intracellular LDH was measured in JCPyV-infected cells at 96 hpt, the number of cells inversely correlated with the artesunate concentration (data not shown) in a similar manner as demonstrated by the resazurin and CellTiter-Glo assays (**Fig.4 D and E**).

We have now shown that artesunate had significant effects on proliferation, DNA replication, metabolic activity and the number of viable mock-infected and JCPyV-infected COS-7 cells. These results could be due to cytostatic effects, cytotoxic effects or a combination of these. In order to investigate potentially cytotoxic effects of artesunate, the CellTox Green Cytotoxicity Assay measuring DNA of dead cells, was performed. The fluorescence signal from accessible DNA was measured at 24, 48, 72 and 96 hpt and normalized to the levels found in untreated mock-infected cells at 24 hpt. At 24 hpt no significant increase in cell death was found for any artesunate concentration in either mock-infected (**Fig.5A**) or JCPyV-infected cells (**Fig.5B**). However, from 48 hpt, artesunate concentrations above 10  $\mu$ M gave increased cell death in both mock-infected and JCPyV-infected cells. At 80  $\mu$ M, respective 5 fold and 4 fold increases in cell death of mock-infected and JCPyV-infected cells were seen. The results were about the same at 72 hpt. At 96 hpt, cell death was more or less doubled independent of the presence of artesunate or virus (**Fig.5A**). Comparing the results from untreated and DMSO treated cells at 96 hpt, the increase in cell death was slightly higher for JCPyV-infected than for mock-infected cells (0.5 and 0.6 fold, respectively) possibly due to lytic effects of JCPyV. For JCPyV-infected cells, the results were confirmed by the use of the Cytotoxicity LDH assay (data not shown).

To summarize the results from the CellTox Green Assay, artesunate concentrations below 20  $\mu$ M did not give significant cytotoxic effects in either mock-infected or JCPyV-infected cells during the 96 hours of treatment. However, artesunate at concentrations of 20  $\mu$ M or higher gave significant toxicity from 48 hpt.

When the results from all cell viability assays were taken together, they suggest that addition of artesunate quickly slowed down or completely stopped cell proliferation in

a concentration-dependent manner. DNA replication and metabolic activity were reduced as early as 24 hpt. However, for artesunate concentrations up to 10  $\mu\text{M}$ , no significant cytotoxicity was observed and the inhibition was transient and was followed by an increase in DNA replication and proliferation compared to untreated cells. Since the DMSO control did not have significant effects on cell viability, all observed effects were assumed to be caused by artesunate and not the solvent.

We conclude that the antiproliferative effect of artesunate on mock-infected and JCPyV-infected COS-7 cells is mainly due to cytostatic effects for concentrations up to and including 10  $\mu\text{M}$  and due to a combination of cytostatic and cytotoxic effects at higher concentrations. Moreover, the infected cells seem to be more sensitive to cytostatic effects than mock-infected cells.

### **Determination of the selective index of artesunate in COS-7 cells**

The therapeutic- or selectivity index (SI) is defined as the ratio of the concentration causing cytotoxicity (CC) versus the concentration giving the desired effect (EC). The SI is usually expressed as  $SI_{50}$ , the ratio of the concentrations giving 50% of the maximum cytotoxic- versus desired- effects ( $CC_{50}/EC_{50}$ ). Since very little toxicity was observed in artesunate treated cells, the  $CC_{50}$  was calculated based on cellular DNA replication of mock-infected cells at 96 hpt (**Fig.4A**) as previously described (43), (37, 44). To estimate the  $EC_{50}$ , the 50% reduction in JCPyV load at 96 hpi, was calculated based on the data in **Fig.2A**. The  $CC_{50}$  was found to be 46  $\mu\text{M}$  (**Fig.6B**) and the  $EC_{50}$  3.0  $\mu\text{M}$  (**Fig.6A**) giving a  $SI_{50}$  ( $CC_{50}/EC_{50}$ ) of 15.

We conclude that artesunate treatment of JCPyV-infected COS-7 cells has a selective index of 15 when a very sensitive method for  $CC_{50}$  calculation was used.

## Discussion

An effective antiviral drug is urgently needed to treat patients with PML which is caused by lytic JCPyV replication in oligodendrocytes. The tried and proven antimalarial drug artesunate had shown broad antiviral effects. We have explored the antiviral activity of artesunate on JCPyV replication in COS-7 cells. The COS-7 cells were selected because of their superior permissivity for JCPyV and stability in cell culture compared to other cell lines tested. The data presented here indicate that artesunate inhibits JCPyV replication in COS-7 cells and that this is connected to a transient cytostatic effect. Artesunate reduced the extracellular JCPyV DNA load at 96 hpi in a concentration-dependent manner, which was verified by a concentration-dependent reduction of infectious progeny. A concentration of 3  $\mu\text{M}$  was calculated to give a 50% inhibition in extracellular JCPyV DNA while 80  $\mu\text{M}$  gave an almost 90% inhibition. The number of cells expressing the late protein VP1, was reduced from 2.5  $\mu\text{M}$  and declining cell numbers were seen at artesunate concentrations from 20  $\mu\text{M}$ . Cell impedance measurements revealed a rapid concentration-dependent inhibition of cell proliferation in both mock-infected and JCPyV-infected cells but for concentrations below 20  $\mu\text{M}$ , the inhibition was only transient. In agreement with this, the DNA replication in mock-infected cells was most strongly affected at 24 hpt and reverted to normal or even higher levels at 96 hpt, at least for concentrations below 40  $\mu\text{M}$ . This was different for JCPyV-infected cells where DNA replication was reduced at 96 hpt. No increase in cell death was detected before 48 hpt, when artesunate concentrations from 20  $\mu\text{M}$  caused increased cell death. A  $\text{SI}_{50}$  of 15 was found using the  $\text{CC}_{50}$  calculated by the sensitive BrdU incorporation assay. This is a more stringent method than that commonly used in the literature, where  $\text{CC}_{50}$  calculation is based on cytotoxicity.

In this study, we found that COS-7 and HEK 293TT cells are highly permissive for JCPyV MAD-4 compared to SVG-A cells. This result is not in line with observations by Ferenczy and colleagues' (46). In their experience, JCPyV replicates better in SVG cells compared to COS-7 cells, but no data was shown. Although HEK 293TT cells apparently can be useful for replication studies of archetype JCPyV and BKPyV (21), the cells detach very easily and could therefore not be used for our study. We used the PML-derived rearranged JCPyV strain MAD-4 but are aware that the enhanced replicative ability of this strain probably played only a minor role due to the constitutive expression of SV40 LTag in COS-7 cells, as previously discussed by Gosert et al (15).

With regard to JCPyV replication, we found that artesunate caused a concentration-dependent reduction in extracellular JCPyV DNA load. Artesunate at 10  $\mu$ M reduced the extracellular JCPyV DNA load at 96 hpi by 75% and this correlated with a decrease in the number of VP1 protein expressing cells and in infectious progeny release. The results are similar to the effects found on replication of BKPyV in RPTECs (37). Here artesunate at 10  $\mu$ M reduced the extracellular BKPyV load at 72 hpi by 65% and a similar reduction in the number of BKPyV-infected cells was seen. For JCPyV replication in COS-7 cells, an  $EC_{50}$  of 3  $\mu$ M was calculated. This is in the same range as found for BKPyV (4.2  $\mu$ M) (37) and for herpesviruses (2.16 – 7.21  $\mu$ M) (27, 29, 47-49). Although artesunate affects a very early stage of herpesvirus infection, the mode of action is still not elucidated (47). In BKPyV-infected RPTECs, artesunate at 10  $\mu$ M inhibited early gene expression but also viral DNA replication, late gene expression and release of progeny virus (37). Since COS-7 cells constitutively express SV40 LTag and there was no specific antibody for JCPyV LTag available, the effect on early protein expression could not be investigated. In contrast

to JCPyV LTag that is only able to drive replication from its own origin, SV40 LTag can initiate viral DNA replication from both the SV40 and JCPyV origin (50). Due to this, a reduction in JCPyV LTag expression in COS-7 cells would probably not have any consequences for viral replication. Since all steps in the replication cycle are connected, inhibition of an early step will inhibit all later steps thereby making it difficult to pinpoint directly affected steps.

With regard to cell viability, artesunate concentrations of 20, 40 and 80  $\mu\text{M}$  visibly reduced the cell numbers. In agreement with this, real time cell analysis demonstrated a rapid concentration-dependent reduction of the cell index in both mock-infected and JCPyV-infected cells which was transient and reversible for concentrations below 20  $\mu\text{M}$ . The results from the BrdU and resazurin assay in mock-infected cells partly supported these findings. For artesunate concentrations up to 20  $\mu\text{M}$ , the inhibitory effect on cellular DNA replication was strongest before 24 hpt and then declined, while the effect on total metabolic activity was also seen from 24 hpt but not reversed up to 96 hpt. One explanation for this apparent discrepancy could be that artesunate arrested the cells in  $G_0$  or  $G_2$ , as previously demonstrated in RPTECs (37) and also in other cells (51-53). When the effect of artesunate waned, a high proportion of the synchronized cells could move into the S-phase incorporating BrdU in their DNA whereas the total metabolic activity was still reduced due to reduced cell numbers in treated wells. For cells treated with artesunate concentrations of 40 and 80  $\mu\text{M}$ , the inhibition of both total metabolic activity and DNA replication seemed to be permanent, the latter probably reflecting a disability in re-entering the cell cycle.



Interestingly, at 96 hpt the DNA replication was more affected in JCPyV-infected cells than in mock-infected cells, especially when concentrations from 10  $\mu$ M were used. The result is opposite from what was found during artesunate treatment of BKPyV-infected RPTECs (37) and is somehow surprising since all COS-7 cells express high levels of SV40 LTag, the key protein stimulating entry into the S-phase during infection (54). Based on the ATP levels, a slightly lower cell number was seen in JCPyV-infected compared to mock-infected wells, but the difference was most pronounced in untreated wells (15%) and could therefore not explain the difference found in DNA replication. That the difference in cell numbers was not seen with the resazurin assay, may be explained by an upregulation of enzymes involved in reduction of resazurin in the infected cells (**Fig.4 D**, untreated cells), similar to that reported in stressed amoeba (55). Since also untreated JCPyV-infected cells showed a 0.5 fold (or 20%) higher cell death than mock-infected cells, the difference in cell numbers probably reflects the lytic effect of the virus. Only when concentrations of 20  $\mu$ M or more were used, did artesunate cause measurable cytotoxic effects. Of note, neurotoxicity has been observed in animal studies when high artesunate concentrations were used but never in humans given recommended doses (56). Taken together our results suggest that artesunate has transient cytostatic effects, in particular on JCPyV-infected COS-7 cells and that only artesunate concentrations from 20  $\mu$ M give cytotoxic effects. Moreover, these results support our findings that artesunate can prevent JCPyV replication and hence the lytic effects in COS-7 cells. The results also indicate that the anti-JCPyV activity of artesunate is based on inhibition of virus-supportive cellular pathways rather than inhibition of a viral target and this is compatible with the cell-based mechanism postulated for the broad anti-herpes virus activity of artesunate (27, 30, 47).

As clearly demonstrated by the real time viability analysis and the BrdU assay, the negative effects on cell viability were transient. This is probably partly explained by the short half life of artesunate and its active metabolite dihydroartemisinin. In one study, the half-life of artesunate in culture medium was 12.4 h in the presence of fibroblast monolayers and 14.4 h without cells present (49). In the same study, dihydroartemisinin had a half-life of 5.2 h in medium without cells. In patients, artesunate has a half-life in plasma of 0.36 or 2.14 h, depending on the route of administration, and dihydroartemisinin of only 0.30 – 1h (reviewed (57)), maybe explaining why side effects are considered to be transient and reversible.

We have now shown that artesunate inhibits the replication of JCPyV in COS-7 cells with an  $EC_{50}$  concentration of 3  $\mu$ M, a concentration that can be achieved in plasma (57-59). However, to be eligible for therapeutic treatment of PML, artesunate also needs to cross the blood-brain barrier and enter the CNS. In one study of six severely sick *Plasmodium falciparum* infected patients treated with intravenous artesunate (approximately 2.3 mg/kg), artesunate was not detectable in CSF samples collected from 15 min to 120 min after injection but only in plasma collected at 15 min (60). However, dihydroartemisinin, was found in plasma and CSF collected at all time points. The concentration in CSF increased over time, while the concentration in plasma decreased over time suggesting that dihydroartemisinin can enter and accumulate in the CSF. Although dihydroartemisinin has a low molecular mass (284 Da) and is highly lipid soluble (61) it is not clear if dihydroartemisinin will reach the affected oligodendrocytes in PML patients. Moreover, longer treatment courses than the usual 7-day treatment regime for malaria (62) may be required for the treatment of PML. Recently two transplant patients with multiresistant CMV received artesunate

for 4 and 7 months without adverse effects while a third patient had to quit treatment after one month due to adverse gastrointestinal effects (33).

In conclusion, artesunate inhibits the replication of JCPyV in COS-7 cells and the antiviral effect appears to be closely related to transient cytostatic drug effects. True cytotoxic effects were exclusively seen at artesunate concentrations from 20  $\mu\text{M}$ , underlining the anti-JCPyV specificity in the low micromolar range. Since the  $\text{EC}_{50}$  of 3  $\mu\text{M}$  can be achieved in plasma of humans and, furthermore, the active metabolite dihydroartemisinin is supposed to accumulate in CSF, artesunate may be useful for the treatment of PML. In the near future, carefully designed clinical studies will have to address pharmacokinetic details of the drug (e.g. penetration into brain) and effects of long-term treatment.

## **Acknowledgments**

We thank Garth D. Tylden for critical reading of the manuscript and helpful comments and Stian Henriksen for his excellent technical support and helpful comments, both at the Department of Microbiology and Infection Control at the University Hospital of North Norway. The project is financially supported by the Northern Norway Regional Health Authority Medical Research Program.

## Figure legends

### **Fig.1. Permissivity of COS-7, HEK 293TT, SVG-A, and M03.13 cells for JCPyV MAD-4.**

The cells were infected with JCPyV MAD-4 for 2 h before the inoculum was replaced with fresh medium. A) Extra- and intracellular JCPyV DNA was quantified by qPCR of supernatants and extracted DNA from cell lysates, respectively, harvested at the indicated time points. Mean values (GEq/ml)  $\pm$  SD of two parallel samples from one representative experiment is presented. B). At four days postinfection, cells were fixed and immunofluorescence staining performed using as primary antibodies polyclonal rabbit anti BKPyV LTag C-terminal serum that cross reacts with SV40 LTag (green) and JCPyV LTag (green) and monoclonal mouse anti JCPyV VP1 (red). The cell nuclei (blue) were stained with Draq5. The pictures were taken with a fluorescence microscope (10X objective).

### **Fig.2. Effect of artesunate on JCPyV replication in COS-7 cells.**

A) Extracellular JCPyV DNA load. At 96 hpi supernatants were harvested from JCPyV-infected COS-7 cells treated with artesunate at the indicated concentrations and JCPyV DNA loads were measured by qPCR. In addition, supernatants were also analyzed at 24 hpi to obtain an input viral load. Mean values (GEq/ml)  $\pm$  SD of three independent experiments (each experiment had two parallel samples) are presented. \*,  $P < 0.05$ , determined by the *t* test.

B) Expression of JCPyV late protein. At 96 hpi, JCPyV-infected COS-7 cells treated with the indicated concentrations of artesunate from 2 hpi were fixed and

immunofluorescence staining performed with the monoclonal mouse anti JCPyV VP1 antibody for visualization of JCPyV late protein VP1 (red) and with Draq5 for the visualization of nuclei (blue). The pictures were taken with a fluorescence microscope (10X objective).

C) Infectious progeny release. The supernatants from untreated and artesunate-treated JCPyV-infected COS-7 cells harvested at 96 hpi were diluted 1:2 in medium and seeded onto new COS-7 cells. At 96 hpi, the cells were fixed and immunostained as described in Fig.2B. The pictures were taken with a fluorescence microscope (X10 objective).

**Fig.3. Effect of artesunate on cell proliferation of mock-infected and JCPyV-infected COS-7 cells in real-time.**

The cells were monitored from the time of seeding upto 96 hpi (A) or 96 hpt (B and C) by a xCELLigence RTCA DP instrument and the adhesion, together with the number and the size of the cells expressed as a cell index. Approximately 24 h post seeding, the cells were infected with conditioned medium or JCPyV for 2 h before the infectious inoculum was removed and replaced by growth medium with or without artesunate at indicated concentrations (for details see material and method).

A) The cell index of mock-infected and JCPyV-infected cells was normalized immediately after infection. The cell index of untreated and artesunate treated B) mock-infected cells and C) JCPyV-infected cells. In B) and C) the cell index was normalized immediately after treatment and the cell index of untreated cells was set as base line 0. The mean values  $\pm$  SD of 3-4 wells (Mock-infected) and of 2 wells (JCPyV-infected) from one representative experiment out of three are shown.

**Fig.4. Cell viability of artesunate-treated mock-infected and JCPyV-infected COS-7 cells.** A) The cellular DNA replication and B) total metabolic activity of mock-infected COS-7 cells was measured at 24, 48, 72 and 96 hpt. C) The cellular DNA replication and D) total metabolic activity of JCPyV-infected COS-7 cells was measured at 96 hpt (98 hpi). E) The ATP content of metabolically active mock-infected and JCPyV-infected COS-7 cells was measured at 96 hpt (98 hpi) (for details see material and methods). Mean values  $\pm$  SD of two to three experiments are presented as the percentage of untreated cells. Each experiment was performed in 3 parallel wells.

**Fig.5. Cytotoxicity of artesunate-treated mock-infected and JCPyV-infected COS-7 cells.** A) Mock-infected and B) JCPyV-infected COS-7 cells were treated with the indicated concentrations of artesunate containing the CellTox Green dye, cyanine from 2 hpi. This dye has an increased fluorescence intensity when bound to DNA of cells with impaired cell membrane. The fluorescence intensity of the dye was measured at 24, 48, 72 and 96 hpt. To correlate the cell death found in artesunate treated cells to that in untreated cells, the fluorescence intensity of each drug concentration measured at all time points was divided by that of untreated mock-infected cells at 24 hpt. Means  $\pm$  SD of two individual experiments are presented as fold changes and each experiment was performed in 3 parallel wells.

**Fig.6. Determination of artesunate EC<sub>50</sub> and CC<sub>50</sub> by curve fitting.** To determine the EC<sub>50</sub> A) and CC<sub>50</sub> B), the effect of increasing concentrations of artesunate on extracellular JCPyV DNA loads and on cellular DNA replication (BrdU incorporation in

Mock-infected cells) was analyzed by curve fitting using the XLfit program. Mean values  $\pm$  SD of three experiments are presented.



## References

1. **Padgett BL, Walker DL, Zurhein GM, Eckroade RJ, Dessel BH.** 1971. Cultivation of papova-like virus from human brain with progressive multifocal leucoencephalopathy. *Lancet* **1**:1257-1260.
2. **Hirsch HH, Kardas P, Kranz D, Leboeuf C.** 2013. The human JC polyomavirus (JCPyV): virological background and clinical implications. *APMIS* **121**:685-727.
3. **Alstadhaug KB, Crougths T, Henriksen S, Leboeu C, Sereti I, Hirsch HH, Rinaldo CH.** 2014. Treatment of Progressive Multifocal 1 Leukoencephalopathy With Interleukin 7, *JAMA Neurology*. In press.
4. **Naess H, Glad S, Storstein A, Rinaldo CH, Mork SJ, Myhr KM, Hirsch H.** 2010. Progressive multifocal leucoencephalopathy in an immunocompetent patient with favourable outcome. A case report. *BMC.Neurol.* **10**:32.
5. **Gheuens S, Pierone G, Peeters P, Koralnik IJ.** 2010. Progressive multifocal leucoencephalopathy in individuals with minimal or occult immunosuppression. *Journal of neurology, neurosurgery, and psychiatry* **81**:247-254.
6. **Egli A, Infanti L, Dumoulin A, Buser A, Samaridis J, Stebler C, Gosert R, Hirsch HH.** 2009. Prevalence of Polyomavirus BK and JC Infection and Replication in 400 Healthy Blood Donors. *J.Infect.Dis.* **199**:837-846.

7. **Knowles WA, Pipkin P, Andrews N, Vyse A, Minor P, Brown DW, Miller E.** 2003. Population-based study of antibody to the human polyomaviruses BKV and JCV and the simian polyomavirus SV40. *J.Med.Virol.* **71**:115-123.
8. **Stolt A, Sasnauskas K, Koskela P, Lehtinen M, Dillner J.** 2003. Seroepidemiology of the human polyomaviruses. *J.Gen.Virol.* **84**:1499-1504.
9. **Chesters PM, Heritage J, Mccance DJ.** 1983. Persistence of DNA sequences of BK virus and JC virus in normal human tissues and in diseased tissues. *J.Infect.Dis.* **147**:676-684.
10. **Monaco MC, Atwood WJ, Gravell M, Tornatore CS, Major EO.** 1996. JC virus infection of hematopoietic progenitor cells, primary B lymphocytes, and tonsillar stromal cells: implications for viral latency. *Journal of virology* **70**:7004-7012.
11. **White FA, 3rd, Ishaq M, Stoner GL, Frisque RJ.** 1992. JC virus DNA is present in many human brain samples from patients without progressive multifocal leukoencephalopathy. *Journal of virology* **66**:5726-5734.
12. **Bayliss J, Karasoulos T, Mclean CA.** 2012. Frequency and large T (LT) sequence of JC polyomavirus DNA in oligodendrocytes, astrocytes and granular cells in non-PML brain. *Brain pathology* **22**:329-336.

13. **Johne R, Buck CB, Allander T, Atwood WJ, Garcea RL, Imperiale MJ, Major EO, Ramqvist T, Norkin LC.** 2011. Taxonomical developments in the family Polyomaviridae. *Archives of virology* **156**:1627-1634.
14. **Trowbridge PW, Frisque RJ.** 1995. Identification of three new JC virus proteins generated by alternative splicing of the early viral mRNA. *Journal of neurovirology* **1**:195-206.
15. **Gosert R, Kardas P, Major EO, Hirsch HH.** 2010. Rearranged JC virus noncoding control regions found in progressive multifocal leukoencephalopathy patient samples increase virus early gene expression and replication rate. *J.Virol.* **84**:10448-10456.
16. **Padgett BL, Rogers CM, Walker DL.** 1977. JC virus, a human polyomavirus associated with progressive multifocal leukoencephalopathy: additional biological characteristics and antigenic relationships. *Infect.Immun.* **15**:656-662.
17. **Gosert R, Rinaldo CH, Wernli M, Major EO, Hirsch HH.** 2011. CMX001 (1-O-Hexadecyloxypropyl-Cidofovir) Inhibits Polyomavirus JC Replication in Human Brain Progenitor-Derived Astrocytes. *Antimicrob.Agents Chemother.* **55**:2129-2136.
18. **Gluzman Y.** 1981. SV40-transformed simian cells support the replication of early SV40 mutants. *Cell* **23**:175-182.

19. **Hara K, Sugimoto C, Kitamura T, Aoki N, Taguchi F, Yogo Y.** 1998. Archetype JC virus efficiently replicates in COS-7 cells, simian cells constitutively expressing simian virus 40 T antigen. *Journal of virology* **72**:5335-5342.
20. **Buck CB, Pastrana DV, Lowy DR, Schiller JT.** 2004. Efficient intracellular assembly of papillomaviral vectors. *Journal of virology* **78**:751-757.
21. **Broekema NM, Imperiale MJ.** 2012. Efficient propagation of archetype BK and JC polyomaviruses. *Virology* **422**:235-241.
22. **Shaw G, Morse S, Ararat M, Graham FL.** 2002. Preferential transformation of human neuronal cells by human adenoviruses and the origin of HEK 293 cells. *FASEB journal : official publication of the Federation of American Societies for Experimental Biology* **16**:869-871.
23. **Major EO, Miller AE, Mourrain P, Traub RG, De Widt E, Sever J.** 1985. Establishment of a line of human fetal glial cells that supports JC virus multiplication. *Proceedings of the National Academy of Sciences of the United States of America* **82**:1257-1261.
24. **Henriksen S, Tylden GD, Dumoulin A, Sharma BN, Hirsch HH, Rinaldo CH.** 2014. The human fetal glial cell line SVG p12 contains infectious BK polyomavirus (BKPyV). *Journal of virology* **88**:7556-7568.

25. **Dondorp AM, Fanello CI, Hendriksen IC, Gomes E, Seni A, Chhaganlal KD, Bojang K, Olaosebikan R, Anunobi N, Maitland K, Kivaya E, Agbenyega T, Nguah SB, Evans J, Gesase S, Kahabuka C, Mtove G, Nadjm B, Deen J, Mwanga-Amumpaire J, Nansumba M, Karema C, Umulisa N, Uwimana A, Mokuolu OA, Adedoyin OT, Johnson WB, Tshefu AK, Onyamboko MA, Sakulthaew T, Ngum WP, Silamut K, Stepniewska K, Woodrow CJ, Bethell D, Wills B, Oneko M, Peto TE, Von Seidlein L, Day NP, White NJ.** 2010. Artesunate versus quinine in the treatment of severe falciparum malaria in African children (AQUAMAT): an open-label, randomised trial. *Lancet* **376**:1647-1657.
  
26. **Romero MR, Efferth T, Serrano MA, Castano B, Macias RI, Briz O, Marin JJ.** 2005. Effect of artemisinin/artesunate as inhibitors of hepatitis B virus production in an "in vitro" replicative system. *Antiviral Res.* **68**:75-83.
  
27. **Auerochs S, Korn K, Marschall M.** 2011. A reporter system for Epstein-Barr virus (EBV) lytic replication: anti-EBV activity of the broad anti-herpesviral drug artesunate. *J.Virol.Methods* **173**:334-339.
  
28. **Romero MR, Serrano MA, Vallejo M, Efferth T, Alvarez M, Marin JJ.** 2006. Antiviral effect of artemisinin from *Artemisia annua* against a model member of the Flaviviridae family, the bovine viral diarrhoea virus (BVDV). *Planta medica* **72**:1169-1174.

29. **Milbradt J, Auerochs S, Korn K, Marschall M.** 2009. Sensitivity of human herpesvirus 6 and other human herpesviruses to the broad-spectrum anti-infective drug artesunate. *J.Clin.Virol.* **46**:24-28.
30. **Efferth T, Romero MR, Wolf DG, Stamminger T, Marin JJ, Marschall M.** 2008. The antiviral activities of artemisinin and artesunate. *Clin.Infect.Dis.* **47**:804-811.
31. **Efferth T, Marschall M, Wang X, Huong SM, Hauber I, Olbrich A, Kronschnabl M, Stamminger T, Huang ES.** 2002. Antiviral activity of artesunate towards wild-type, recombinant, and ganciclovir-resistant human cytomegaloviruses. *J.Mol.Med.* **80**:233-242.
32. **Shapira MY, Resnick IB, Chou S, Neumann AU, Lurain NS, Stamminger T, Caplan O, Saleh N, Efferth T, Marschall M, Wolf DG.** 2008. Artesunate as a potent antiviral agent in a patient with late drug-resistant cytomegalovirus infection after hematopoietic stem cell transplantation. *Clin.Infect.Dis.* **46**:1455-1457.
33. **Germi R, Mariette C, Alain S, Lupo J, Thiebaut A, Brion JP, Epaulard O, Saint Raymond C, Malvezzi P, Morand P.** 2014. Success and failure of artesunate treatment in five transplant recipients with disease caused by drug-resistant cytomegalovirus. *Antiviral research* **101**:57-61.
34. **Hakacova N, Klingel K, Kandolf R, Engdahl E, Fogdell-Hahn A, Higgins T.** 2013. First therapeutic use of Artesunate in treatment of human herpesvirus

- 6B myocarditis in a child. *Journal of clinical virology : the official publication of the Pan American Society for Clinical Virology* **57**:157-160.
35. **Wolf DG, Shimoni A, Resnick IB, Stamminger T, Neumann AU, Chou S, Efferth T, Caplan O, Rose J, Nagler A, Marschall M.** 2011. Human cytomegalovirus kinetics following institution of artesunate after hematopoietic stem cell transplantation. *Antiviral research* **90**:183-186.
  36. **Lau PK, Woods ML, Ratanjee SK, John GT.** 2011. Artesunate is ineffective in controlling valganciclovir-resistant cytomegalovirus infection. *Clinical infectious diseases : an official publication of the Infectious Diseases Society of America* **52**:279.
  37. **Sharma BN, Marschall M, Henriksen S, Rinaldo CH.** 2014. Antiviral effects of artesunate on polyomavirus BK replication in primary human kidney cells. *Antimicrobial agents and chemotherapy* **58**:279-289.
  38. **Mclaurin J, Trudel GC, Shaw IT, Antel JP, Cashman NR.** 1995. A human glial hybrid cell line differentially expressing genes subserving oligodendrocyte and astrocyte phenotype. *Journal of neurobiology* **26**:283-293.
  39. **Padgett BL, Walker DL, Zurhein GM, Hodach AE, Chou SM.** 1976. JC Papovavirus in progressive multifocal leukoencephalopathy. *The Journal of infectious diseases* **133**:686-690.

40. **Schweighardt B, Shieh JT, Atwood WJ.** 2001. CD4/CXCR4-independent infection of human astrocytes by a T-tropic strain of HIV-1. *Journal of neurovirology* **7**:155-162.
41. **Drachenberg CB, Hirsch HH, Papadimitriou JC, Gosert R, Wali RK, Munivenkatappa R, Nogueira J, Cangro CB, Haririan A, Mendley S, Ramos E.** 2007. Polyomavirus BK versus JC replication and nephropathy in renal transplant recipients: a prospective evaluation. *Transplantation* **84**:323-330.
42. **Hey AW, Johnsen JI, Johansen B, Traavik T.** 1994. A two fusion partner system for raising antibodies against small immunogens expressed in bacteria. *J.Immunol.Methods* **173**:149-156.
43. **Rinaldo CH, Gosert R, Bernhoff E, Finstad S, Hirsch HH.** 2010. 1-O-hexadecyloxypropyl cidofovir (CMX001) effectively inhibits polyomavirus BK replication in primary human renal tubular epithelial cells. *Antimicrob.Agents Chemother.* **54**:4714-4722.
44. **Sharma BN, Li R, Bernhoff E, Gutteberg TJ, Rinaldo CH.** 2011. Fluoroquinolones inhibit human polyomavirus BK (BKV) replication in primary human kidney cells. *Antiviral Res.* **92**:115-123.
45. **Schowalter RM, Buck CB.** 2013. The Merkel cell polyomavirus minor capsid protein. *PLoS pathogens* **9**:e1003558.



46. **Ferenczy MW, Marshall LJ, Nelson CD, Atwood WJ, Nath A, Khalili K, Major EO.** 2012. Molecular biology, epidemiology, and pathogenesis of progressive multifocal leukoencephalopathy, the JC virus-induced demyelinating disease of the human brain. *Clinical microbiology reviews* **25**:471-506.
47. **Chou S, Marousek G, Auerochs S, Stamminger T, Milbradt J, Marschall M.** 2011. The unique antiviral activity of artesunate is broadly effective against human cytomegaloviruses including therapy-resistant mutants. *Antiviral Res.* **92**:364-368.
48. **Efferth T, Kaina B.** 2010. Toxicity of the antimalarial artemisinin and its derivatives. *Crit Rev.Toxicol.* **40**:405-421.
49. **Flobinus A, Taudon N, Desbordes M, Labrosse B, Simon F, Mazon MC, Schnepf N.** 2014. Stability and antiviral activity against human cytomegalovirus of artemisinin derivatives. *The Journal of antimicrobial chemotherapy* **69**:34-40.
50. **Lynch KJ, Frisque RJ.** 1990. Identification of critical elements within the JC virus DNA replication origin. *J.Virol.* **64**:5812-5822.
51. **Jiang Z, Chai J, Chuang HH, Li S, Wang T, Cheng Y, Chen W, Zhou D.** 2012. Artesunate induces G0/G1 cell cycle arrest and iron-mediated mitochondrial apoptosis in A431 human epidermoid carcinoma cells. *Anticancer Drugs* **23**:606-613.

52. **Li S, Xue F, Cheng Z, Yang X, Wang S, Geng F, Pan L.** 2009. Effect of artesunate on inhibiting proliferation and inducing apoptosis of SP2/0 myeloma cells through affecting NFkappaB p65. *International journal of hematology* **90**:513-521.
53. **Xu Q, Li ZX, Peng HQ, Sun ZW, Cheng RL, Ye ZM, Li WX.** 2011. Artesunate inhibits growth and induces apoptosis in human osteosarcoma HOS cell line in vitro and in vivo. *Journal of Zhejiang University. Science. B* **12**:247-255.
54. **Sullivan CS, Pipas JM.** 2002. T antigens of simian virus 40: molecular chaperones for viral replication and tumorigenesis. *Microbiol.Mol.Biol.Rev.* **66**:179-202.
55. **Hereder-Bermejo I, Copa-Patino JL, Soliveri J, Gomez R, De La Mata FJ, Perez-Serrano J.** 2013. In vitro comparative assessment of different viability assays in *Acanthamoeba castellanii* and *Acanthamoeba polyphaga* trophozoites. *Parasitology research* **112**:4087-4095.
56. **Manning L, Laman M, Page-Sharp M, Salman S, Hwaiwhanje I, Morep N, Siba P, Mueller I, Karunajeewa HA, Davis TM.** 2011. Meningeal inflammation increases artemether concentrations in cerebrospinal fluid in Papua New Guinean children treated with intramuscular artemether. *Antimicrobial agents and chemotherapy* **55**:5027-5033.
57. **Morris CA, Duparc S, Borghini-Fuhrer I, Jung D, Shin CS, Fleckenstein L.** 2011. Review of the clinical pharmacokinetics of artesunate and its active

metabolite dihydroartemisinin following intravenous, intramuscular, oral or rectal administration. *Malaria journal* **10**:263.

58. **Li Q, Cantilena LR, Leary KJ, Saviolakis GA, Miller RS, Melendez V, Weina PJ.** 2009. Pharmacokinetic profiles of artesunate after single intravenous doses at 0.5, 1, 2, 4, and 8 mg/kg in healthy volunteers: a phase I study. *The American journal of tropical medicine and hygiene* **81**:615-621.
59. **Miller RS, Li Q, Cantilena LR, Leary KJ, Saviolakis GA, Melendez V, Smith B, Weina PJ.** 2012. Pharmacokinetic profiles of artesunate following multiple intravenous doses of 2, 4, and 8 mg/kg in healthy volunteers: phase 1b study. *Malaria journal* **11**:255.
60. **Davis TM, Binh TQ, Ilett KF, Batty KT, Phuong HL, Chiswell GM, Phuong VD, Agus C.** 2003. Penetration of dihydroartemisinin into cerebrospinal fluid after administration of intravenous artesunate in severe falciparum malaria. *Antimicrobial agents and chemotherapy* **47**:368-370.
61. **Kearney BP, Aweeka FT.** 1999. The penetration of anti-infectives into the central nervous system. *Neurologic clinics* **17**:883-900.
62. **Bethell D, Se Y, Lon C, Tyner S, Saunders D, Sriwichai S, Darapiseth S, Teja-Isavadharm P, Khemawoot P, Schaecher K, Ruttvisutinunt W, Lin J, Kuntawungin W, Gosi P, Timmermans A, Smith B, Socheat D, Fukuda MM.** 2011. Artesunate dose escalation for the treatment of uncomplicated

malaria in a region of reported artemisinin resistance: a randomized clinical trial. PloS one **6**:e19283.

Figure 1

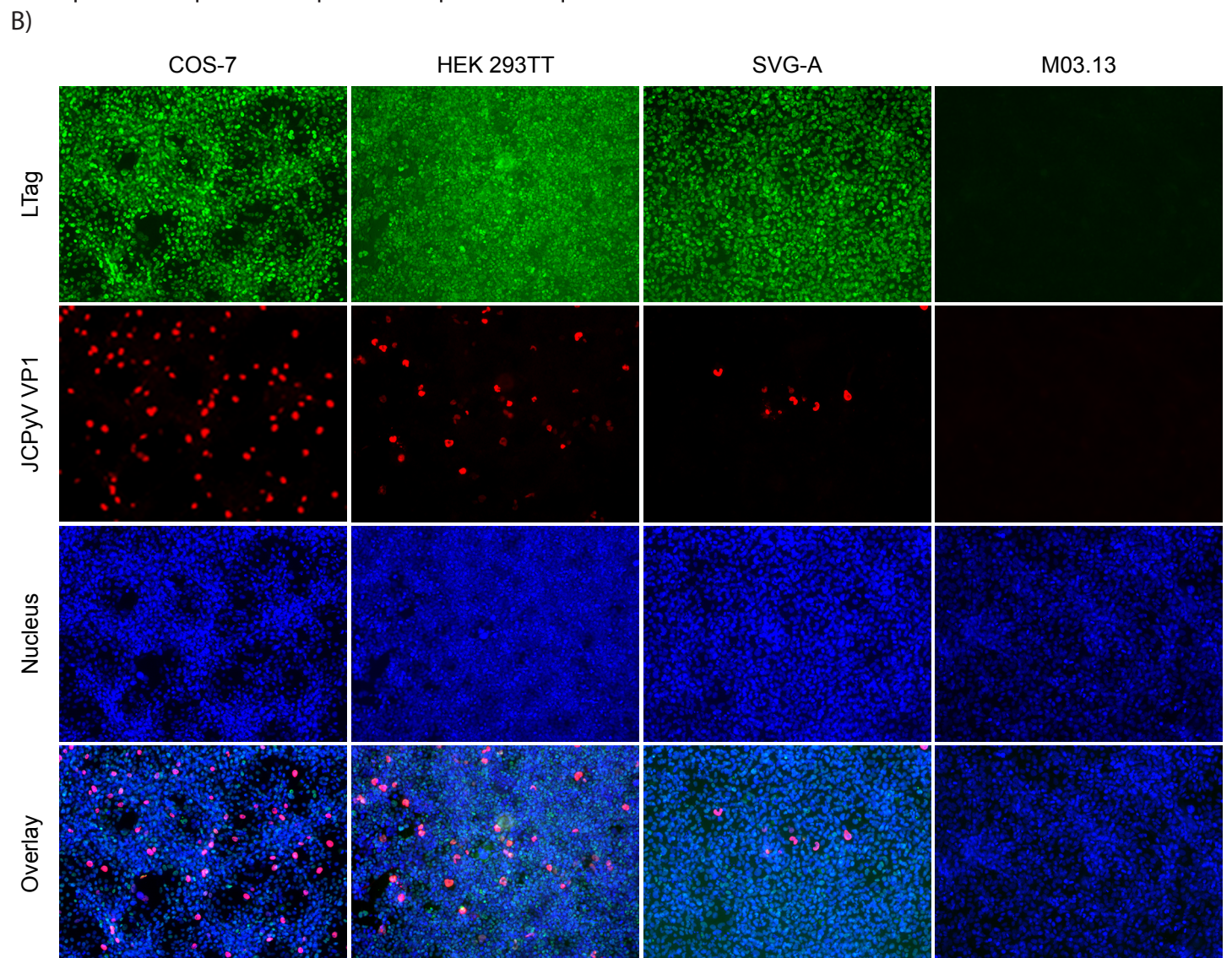
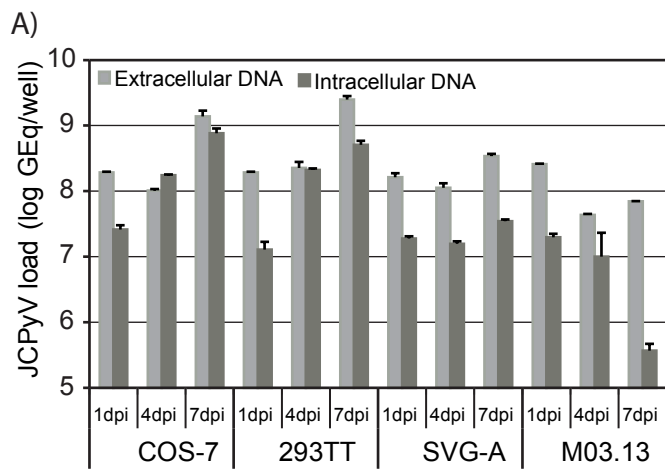


Figure 2

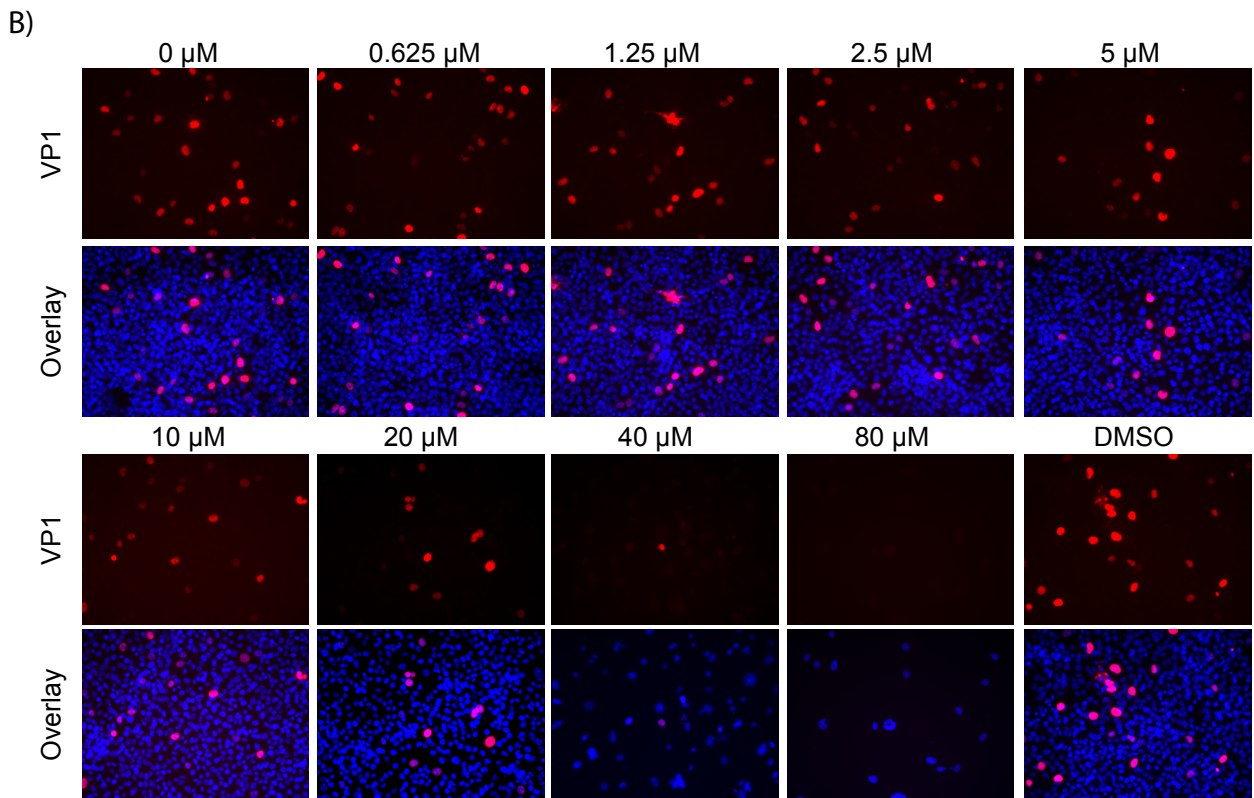
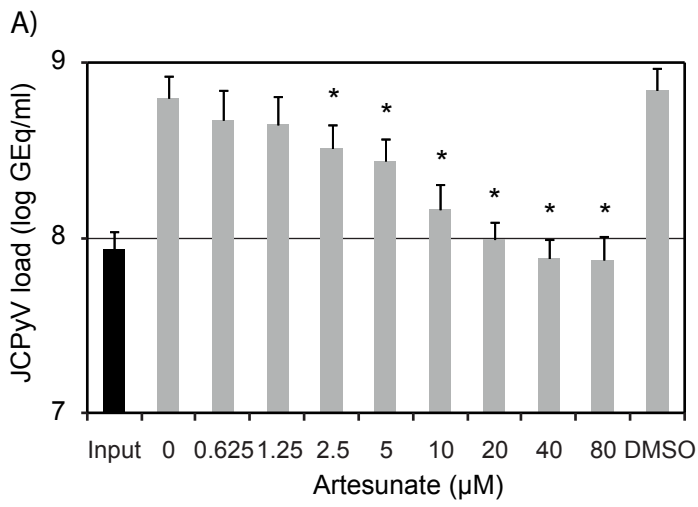


Figure 2

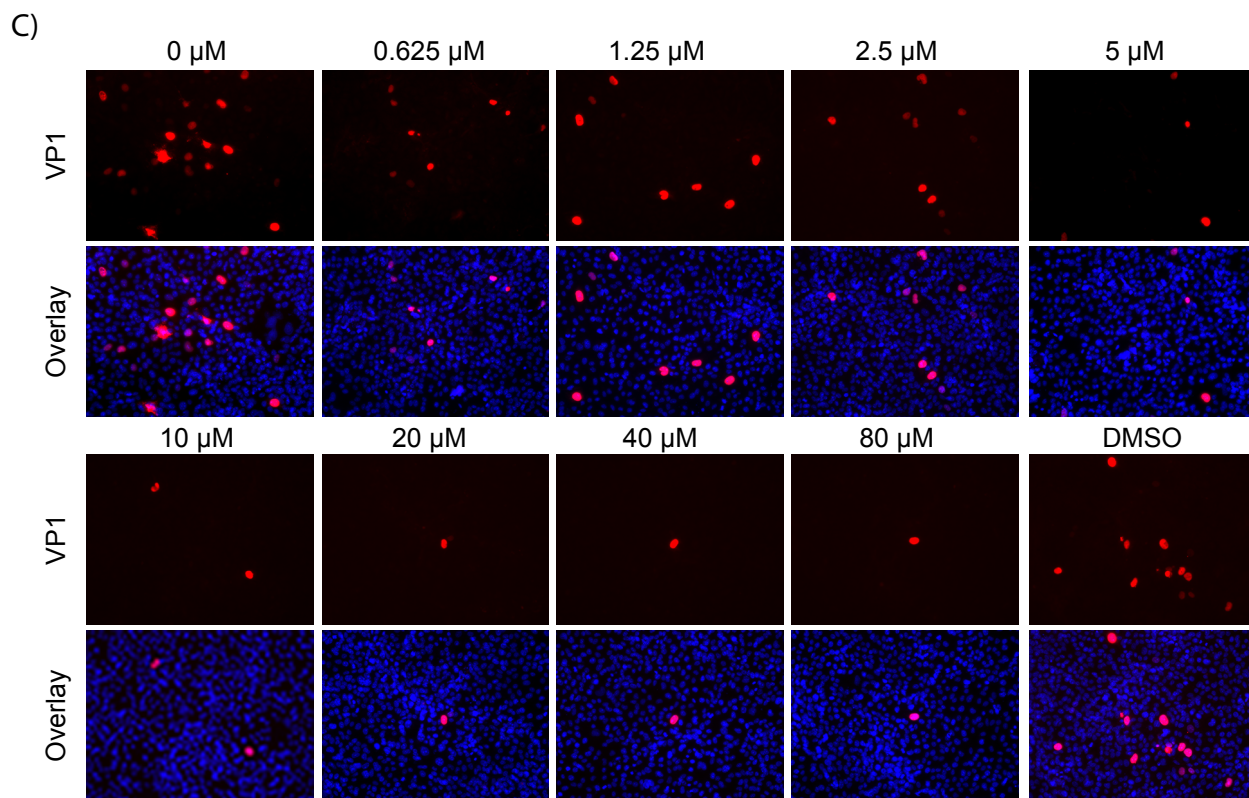


Figure 3

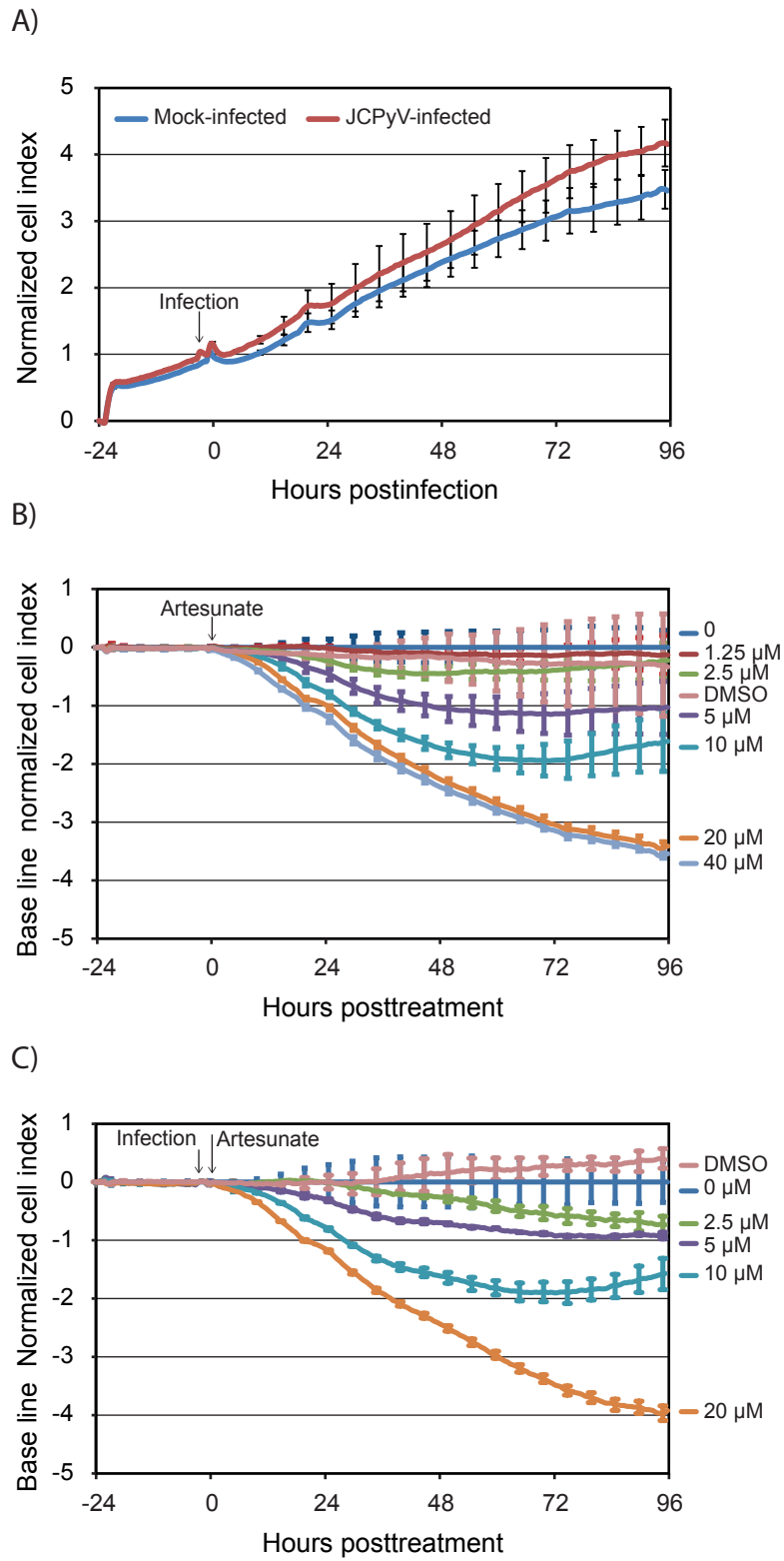




Figure 4

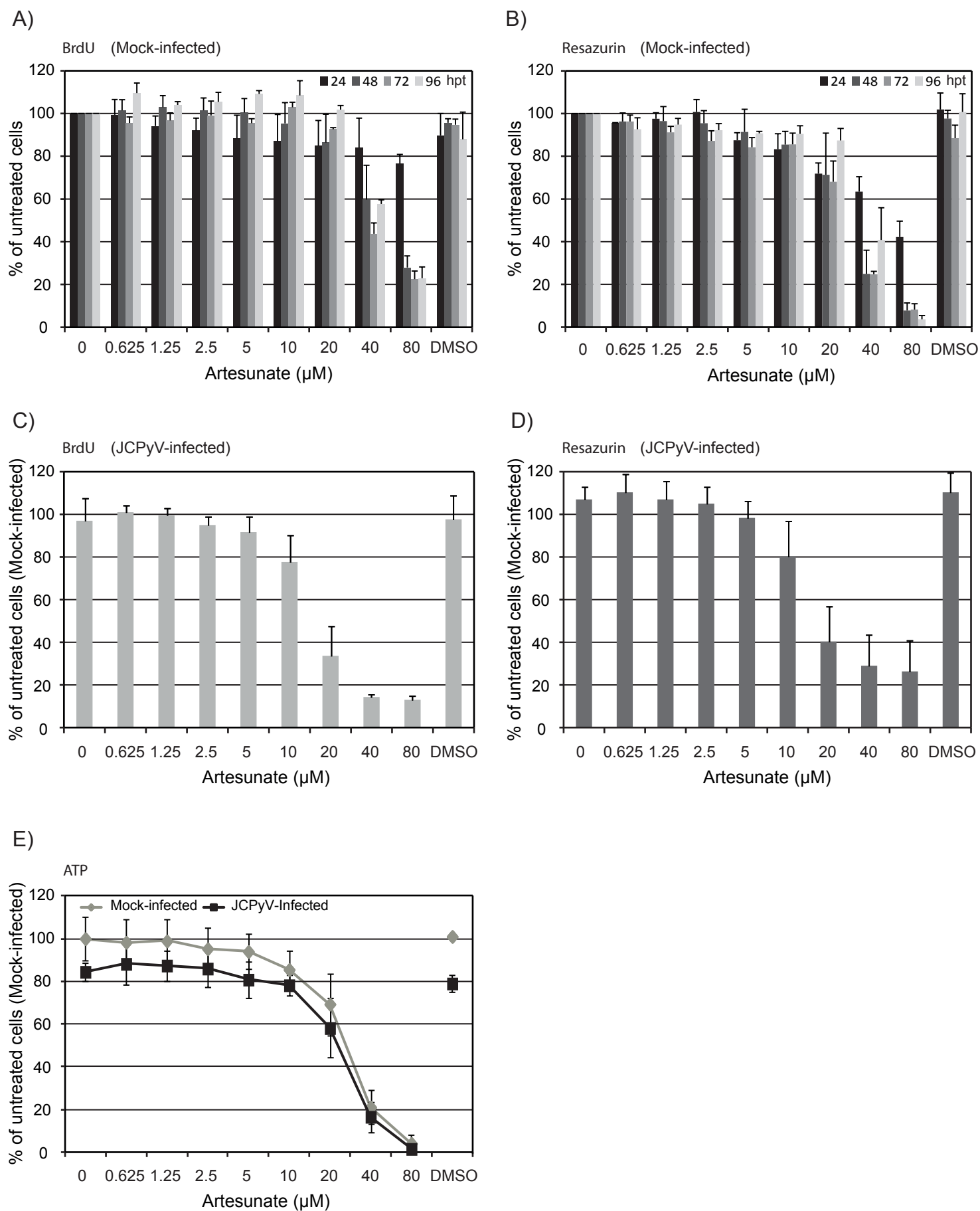


Figure 5

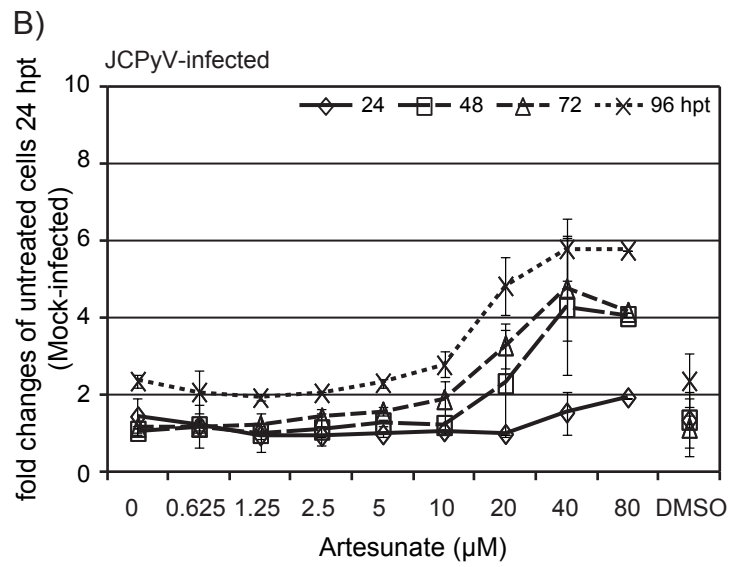
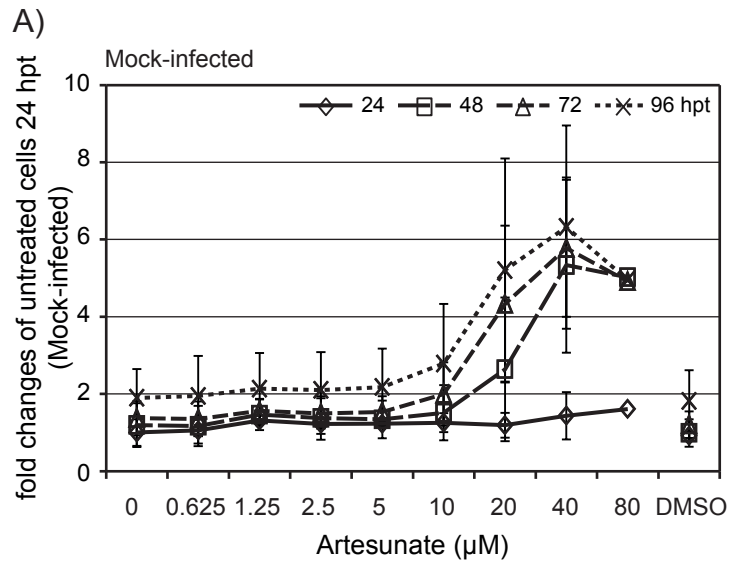
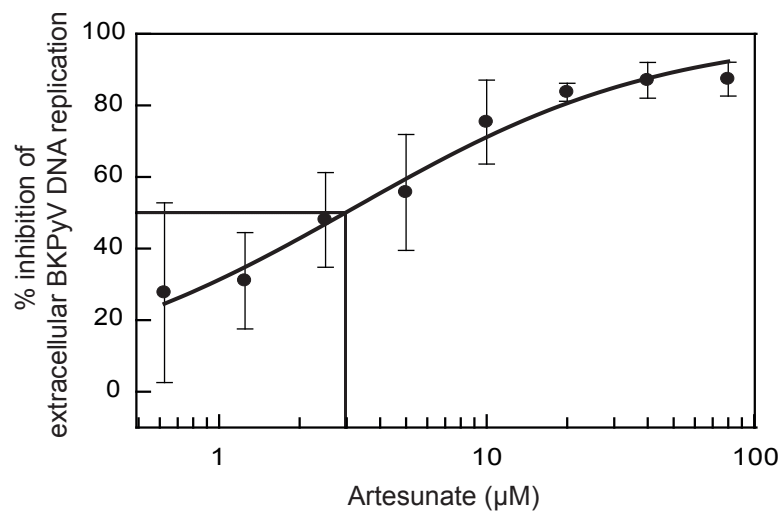


Figure 6

A)



B)

